Broadband colored-crescent generation in a single β-barium-borate crystal by intense femtosecond pulses

L. Wang,[1] Y. X. Fan,[1] H. Zhu,[1] Z. D. Yan,[1] H. Zeng,[2] H.-T. Wang,[1,3] S. N. Zhu,[1] and Z. L. Wang[1,*]

[1]*Department of Physics and National Laboratory of Solid State Microstructures, Nanjing University, 210093 Nanjing, China*

[2]*State Key Laboratory of Precision Spectroscopy, East China Normal University, 200062 Shanghai, China*

[3]*School of Physics, Nankai University, 300071 Tianjin, China*

(Received 24 April 2011; published 13 December 2011)

A visible colored crescent with a bandwidth broader than 220 nm is observed experimentally by loosely focused femtosecond pulses in a bulk quadratic nonlinear crystal (β-BBO crystal) at certain incident angles. Through the analysis based on a simple collinear phase-matching model, we suggest that the colored crescent might be the coexistence of spontaneous parametric down-conversions (SPDCs) in the infrared range and the corresponding efficient second-order harmonic generations (SHGs) that occur in a wide spectrum. We further provide a possible mechanism for the SHG process in which the phase-mismatching angles of the frequency doubling of SPDCs in β-BBO crystal are assumed to be compensated by the strong diffraction effect during the self-focusing process of the generated intense SPDC signals.

DOI: 10.1103/PhysRevA.84.063831 PACS number(s): 42.65.Ky, 42.65.Hw, 42.65.Lm

I. INTRODUCTION

The propagation of intense femtosecond pulses through a quadratic nonlinear crystal can give rise to interesting nonlinear frequency conversion phenomena. For example, second- and third-order harmonic generations [1,2], sum-frequency generation [3,4], multistep parametric processes [5], optical parametric amplification [6,7], anti-Stoke Raman scattering [8], and spatial solitons [9] have been observed experimentally. Meanwhile, when intense light propagates in a transparent medium including quadratic nonlinear crystals, modulation instability usually occurs due to the interplay of optical Kerr nonlinearity and group velocity dispersion or diffraction, producing an exponential growth of perturbations during photon-medium interactions [10]. For example, away from phase-matching conditions of second-harmonic generation (SHG), BBO and KDP crystals could produce white-light supercontinuum (WLSC) in the center of the beam and colored conical emission (CCE) rings surrounding the white core [11,12]. Interestingly, when the phase-matching condition for SHG is satisfied, the spatiotemporally coupled modulation instability in a quadratic crystal can result in a series of bright cyan rings [13–15]. The generated broadband tunable correlated photons [16] could have potential applications in quantum network [17], quantum memory [18], etc. In addition, ultrabroadband parametric down-conversion and octave-spanning spectra generation in quadratic media have also been explored by experiments [19,20] and numerically simulated using a single-wave envelope equation [21,22], which is helpful to analyze various supercontinuum phenomena.

In this paper, we report the observation of a visible colored crescent by illuminating intense femtosecond pulses into a β-BBO crystal at certain incident angles under a loose focusing condition. By comparing the experimental results with the calculations that are based on a simple model of collinear phase-matching conditions, we suggest that the colored crescent observed here might be a result of an efficient SHG conversion from spontaneous parametric down-conversion (SPDC) generated in the nonlinear crystal. The diffraction effect during self-focusing [23] is suggested as one of the possible mechanisms to make part of the generated SPDC signal fulfill the phase-matching conditions for frequency doublings in a wide optical spectrum and produce broadband (more than 220-nm bandwidth) parametric upconverted signals in the visible range.

II. EXPERIMENTAL SETUP

In the experiment, the pump source was a 1 kHz Ti:sapphire regeneratively amplified femtosecond laser system (Legend-Elite, Coherent Inc.), which produced 40-fs pulses at a center wavelength of 800 nm with an average power of 2.5 W. The output pulses were polarized in the x-y plane in which the optical axis of the β-BBO crystal was located (see Fig. 1). The laser beam diameter was set to 1 mm by an iris and the intensity was varied by adjusting a neutral-density (ND) filter, which was placed after the iris. Then the laser pulses were focused into a 10-mm-long β-BBO crystal (type-I, $\theta_0 = 27.5^\circ$ cut) by a lens of 500-mm focal length. The incident angle (θ) was changed by rotating the crystal around the z axis, which was perpendicular to the x-y plane. The images of the light emitted from the BBO crystal were projected on a white screen and recorded by a digital camera. Output spectrum in the visible part ($\lambda < 720$ nm) collected by a lens was measured by a spectrometer (USB4000, Ocean Optics). The residual near-infrared signals in the spectrum range from 720 nm to 1200 nm was blocked by an interference filter. It is noteworthy that maximum type-I SHG yield from the pump and bright cyan rings have been observed when the pump is polarized along the z axis for certain incident angles [14]. In our experimental setup, the incident pump was polarized in the x-y plane, which does not satisfy the phase-matching requirement [14], and thus the generated weak type-I SHG plays a negligible role for the phenomenon observed in our experiment, which will be discussed in what follows.

*zlwang@nju.edu.cn

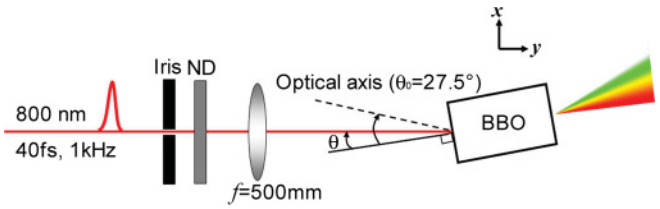

FIG. 1. (Color online) Schematic of experimental setup (top view).

III. EXPERIMENTAL RESULTS AND DISCUSSION

In our experiment, it is observed that when rotating the β-BBO crystal around the z axis, a colored crescent is generated at certain incident angles (θ). The input pulse energy is 30 μJ. The red and narrow crescent begins to appear when the incident angle is increased to the vicinity of $\theta = 8^\circ$, as is shown in Fig. 2(a). The colored crescent is observed to have the following characteristics: its intensity at the outer edge with a shorter wavelength is weaker than that of the inner part. Upon increasing the incident angle to the region from 8° to 12°, the crescent spatial width gradually broadens and finally evolves into a near semicircle at $\theta = 12^\circ$. The crescent color covers the red-green spectrum range and its overall amplitude reaches its maximum in brightness near $\theta = 12^\circ$. Once the incident angle is increased beyond 12°, the colored pattern size begins to shrink and finally vanishes beyond $\theta = 13^\circ$. Note that the SHG conversion efficiency of the pump is very low in all these cases, because neither the pump polarization nor the incident angle is satisfied for the phase-matching condition (pump polarization along the z axis and $\theta = -2^\circ$, as was measured in our experiment). Thus any SPDC in the form of bright colored rings due to the SHG from the pump can be neglected [24]. A bright tiny spot is always observed in the center of the images in Fig. 2(a). This is the SHG due to a phase-locking process [25–29] in which the pump traps portions of its harmonics without walk-offs for the pulses.

The continuous spectra of these colored crescents in the visible range are recorded at different incident angles and shown in Fig. 2(b). With the gradual increase of the incident angle from 8° to 12°, the spectrum blue-shifts and its total intensity is found to increase, reaching its maximum near $\theta = 12^\circ$. In Fig. 2(b), steep declines appearing around 720 nm are due to the pass-band edge of the filter used. Although the near-infrared signals have been blocked from the spectra by the filter, the residual bandwidth observed at $\theta = 12^\circ$ is still broader than 220 nm in the visible range. With further increase of the incident angle beyond 12°, however, the crescent intensity is observed to drop rapidly [see the black dash-dotted curve at 13° in Fig. 2(b)].

Besides the condition of a proper range of incident angles discussed above, an appropriate focusing condition and sufficient pump power are important for the generation of the colored crescent. For example, for a loose focusing condition case (the focal length of the lens $f = 500$ mm), the energy threshold for the occurrence of the colored crescent is about 11 μJ at $\theta = 12^\circ$. When the input pulse energy is increased above 35 μJ, the intense pulses produce WLSC in the center and surrounding colored conical rings, signaling the occurrence of filamentation [10,30]. WLSC could be explained as ionization-enhanced self-phase-modulation [31–34], while colored conical emission rings could be attributed to a number of mechanisms, including four-wave mixing [35], Cherenkov radiation [30], X-wave interpretation [36], as well as the intrinsic second-order nonlinearity and spatiotemporal modulation instability in quadratic materials [13,14]. Since the WLSC is independent of the incident angles, the pump incident angle is set to be $\theta = 0^\circ$ to suppress the generation of colored-crescent emission and to characterize the WLSC itself. As shown in Fig. 2(c), the observed WLSC shows a much wider spectrum and its intensity is quite weak.

In our experiment, the colored crescent can be generated more easily under a loose focusing condition ($f = 500$ mm). In this case, the energy threshold for the occurrence of the colored crescent was about 11 μJ, while that of WLSC is 35 μJ. Under a tighter focusing condition (i.e., $f = 150$ mm) WLSC are generated first because its threshold pump energy (~1 μJ) is much lower than that of the colored crescent (~7 μJ). On the other hand, the colored crescent becomes too weak to be observed due to the low pump intensities with the longer lens focusing length or even the removal of the lens. These observations imply that a loose

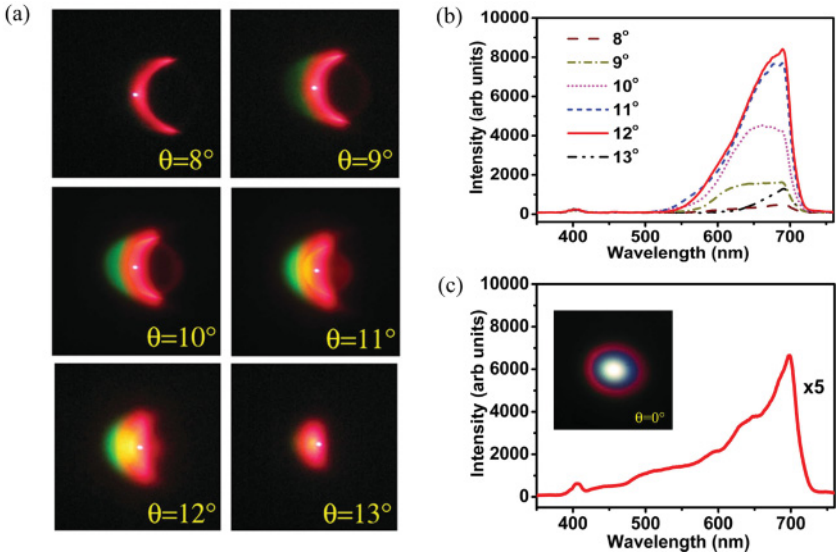

FIG. 2. (Color online) Images (a) and spectra (b) of the colored crescents measured at different incident angles in the range from 8–13°. The input pulse energy was fixed to be 30 μJ. (c) Measured spectrum of the white-light supercontinuum and colored conical emission rings at a normal incidence of loosely focused femtosecond pulses ($\theta = 0^\circ$) and the recorded image (inset).

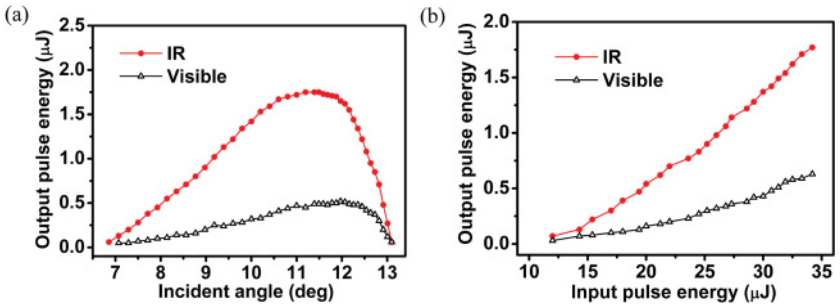

FIG. 3. (Color online) The visible and IR pulse energy from the BBO crystal as functions of the incident angle (a) and the input pulse energy (b). The input pump pulse energy is 30 μJ for (a). The incident angle is 12° for (b).

focusing condition and enough pump power are essential for the colored-crescent generation. Therefore, the following experimental results are obtained under the loose focusing condition ($f = 500$ mm).

In addition to the colored crescent, there is a strong IR signal from the BBO crystal, which can be evidenced experimentally using an IR card or through a frequency-doubling process using another BBO crystal. We observed a broadened ring of the IR signal in the far field on an IR card, which is illustrated as an inset of Fig. 4(a). It is observed that the frequency-doubling spectrum of the IR signal covers the range from 600 nm to 1000 nm or even longer (results not shown here), indicating that the corresponding IR signals should be extended at least from 1200 nm to 2000 nm in the spectrum. The visible and the IR output pulse energies are measured as functions of the incident angle and presented in Fig. 3(a). An energy of 30 μJ of the input pump pulse is fixed in this measurement. In our experiment, a stop-band filter (720 nm $< \lambda <$ 1200 nm) is used to block the strong residual pump signal [i.e., the visible part ($\lambda <$ 720 nm) and IR part ($\lambda >$ 1200 nm) can pass through this filter]. The energy of the visible part is obtained by subtracting the IR part that is recorded by another long-pass filter from the total output pulse energy. From Fig. 3(a), it is seen that the visible output increases steadily after the incident angle is increased beyond $\theta = 7°$, reaching its maximum at $\theta = 12°$. For $\theta > 12°$, the visible output decreases rapidly, and vanishes at $\theta = 13°$. Although the IR output part dependence shows the same trend as the visible output, its intensity is much higher, attaining a maximum at $\theta = 11.5°$. Figure 3(b) plots the dependencies of the measured visible and IR outputs on the input pump pulse energy, from which a nearly linear dependence is observed for both outputs. We further confirm experimentally that the colored crescent (visible part, $\lambda <$ 720 nm) has the same polarization state as that of the pump light (polarized in the x-y plane), whereas the IR part ($\lambda >$ 1200 nm) is polarized along the z axis.

Considering the quite similar dependence of the output visible and IR radiations on the pump incident angle and pulse energy, we propose that the observed colored crescent is a manifestation of the efficient SHG conversion from the generated SPDC. Recently, the SPDC under a strongly focused pump has been studied, and a broadening effect of the far-field SPDC ring has been found, which is explained as a result of the transverse momentum spreading, making the phase-matching range extend beyond that for the initial focused pump beam [37,38]. In our experiment, the generated SPDC peak intensity is estimated to be on the order of 100 GW/cm^2, exceeding the critical intensity for self-focusing in the BBO crystal or even approaching the minimum intensity required for WLSC generation [12]. It is thus expected that in our experiment, the intense femtosecond pulses are subject to self-focusing from optical Kerr nonlinearity [23]. As a consequence, the spatial frequency or the transverse momentum of the SPDC could be largely broadened with a divergent angle during the self-focusing process and efficient frequency-doubling conversions are thus expected. The inset in Fig. 4(a) shows the far-field intensity profile of broadened SPDC on an IR card as a result of the transverse momentum spreading in our experiment.

We further assume that the vertically (along the z axis) polarized IR is attributed to type-I ($e \rightarrow o + o$) SPDC of the pump at 800 nm, and the horizontally (in the x-y plane) polarized visible output is attributed to type-I ($o + o \rightarrow e$) SHG of this generated SPDC. Our assumptions are reasonable and can be supported by calculating the phase-matching angle α_{SPDC} for the IR signal or idle signal and α_{SHG} for the SHG of SPDC under a conventional plane-wave approximation according to collinear momentum and energy conservations [23]. The calculated values for α_{SPDC} and α_{SHG} are plotted as functions of the SPDC wavelength in Fig. 4(b). The corresponding incident angle of the pump is also calculated and labeled on the right axis in Fig. 4(b). According to the calculations, the SPDC and its SHG usually have different phase-matching angles. However, the predicted angle mismatch $\Delta\alpha = \alpha_{\mathrm{SHG}} - \alpha_{\mathrm{SPDC}}$ is smaller than 2° for the SPDC wavelength in the range from 1100 nm to 2100 nm and approach zero around a wavelength of

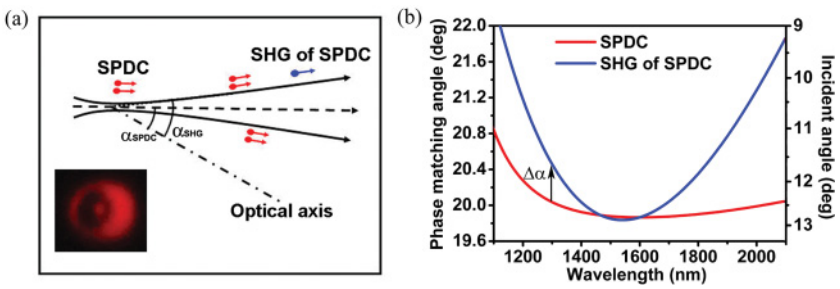

FIG. 4. (Color online) (a) Schematic of SPDC diffraction and its SHG in a BBO crystal. Inset: a far-field intensity profile of SPDC on an IR card. (b) Calculated phase-matching angles for the SPDC and its SHG in the crystal. The corresponding incident angle of the pump is also shown on the right axis.

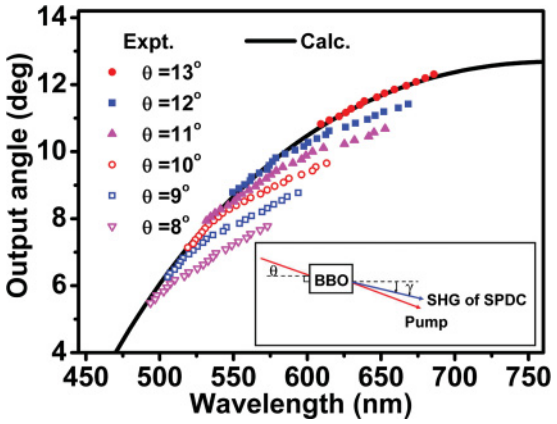

FIG. 5. (Color online) Calculated (black solid curve) SHG output angles (γ) and measured results as functions of SHG wavelength at different incident angles.

1600 nm. This means that an efficient parametric conversion of the intense fundamental wave as well as the SHG of the SPDC could be realized when the SPDC wavelength is tuned around 1600 nm under a proper angle of incidence of the fundamental wave. This is in good agreement with our experimental results in Fig. 2(b) in which the measured intensity of the signal in the visible spectrum is observed to increase from a wavelength of 500 nm and begins to saturate when its wavelength approaches 720 nm beyond which the signal was blocked by the filter used. Although $\Delta\alpha$ begins to increase gradually as the wavelength is tuned away from 1600 nm, a strong diffraction effect could satisfy the phase-matching conditions of the two processes simultaneously, leading to efficient parametric conversions of the intense fundamental wave as well as the SHG of the SPDC in a broadband spectrum regime [Fig. 4(a)]. On the other hand, because α_{SHG} is larger than α_{SPDC}, only the portion of the SPDC that is diffracted to the phase-matching directions can be converted to its SHG efficiently. This explains the appearance of colored crescents observed in our experiment, which are noncentrosymmetric [Fig. 2(a)].

The observed colored crescent is suggested to be a SHG of the SPDC signal assisted by the self-focusing induced diffraction of the generated high-intense SPDC in a BBO crystal. This can be further supported by comparing the measured and calculated SHG output angles γ (the angle between the SHG signal and the normal line of the crystal output surface) as functions of the SHG wavelength. The SHG output angle versus SHG wavelength under different incident angles is measured and summarized in Fig. 5. The black solid curve in Fig. 5 is the calculated output angles that satisfy the phase-matching condition and energy conservation for SHG [23], not taking into account the diffraction effect of the intense SPDC. As is seen, the measured SHG output angles for each incident angle fit the calculation curve at short wavelengths very well. Deviations between experiment and the calculation based on the simplified model become large at longer wavelengths for which the calculated SHG propagation direction approaches that of the pump. Such deviations are attributed to the influence from the intense pump, the potential mechanism includes the cross-phase-modulation due to pump and SHG coupling [39], parametric scattering [40,41], etc., which were not considered in our calculations. At the incident angle $\theta = 13^\circ$, the calculated SHG propagation direction is far from that of the pump and the generated SHG intensity is much weaker than other incident angles [Fig. 1(b)]. Thus the weak coupling between the SHG and the pump can explain a good fitting between the experimental results and the calculation at the incident angle $\theta = 13^\circ$ as well as the short-wavelength side of other angles. Full three-dimensional numerical calculations are needed to reveal the full picture of these phenomena.

IV. CONCLUSION

A visible colored crescent is generated experimentally in a 10-mm-long quadratic nonlinear crystal by intense femtosecond pulses. We propose that the colored crescent might be due to the occurrence of SPDC of the fundamental wave and the SHG of the intense SPDC signal. Considering the small difference for their phase-matching angles based on a simple collinear phase-matching model, we think that a simultaneous realization for a type-I phase matching of SPDC and its SHG is a reasonable picture for the observed phenomenon, by assuming that the generated SPDC could be diffracted to the SHG phase-matching angle during the self-focusing process in the crystal. Our analysis does not exclude other possible nonlinear interactions that could contribute to the presence of the colored crescent, such as cascaded second-order processes [42], noncollinear phase matching [43], and self-phase-modulation [44]. Our study provides an approach to achieve broadband SHG from the monochromatic pump, and may stimulate some potential applications to realize broadband tunable optical parametric up-converted amplification as well as to characterize the intrinsic physical processes and mechanisms of nonlinear optical parametric scattering in quadratic media under the excitation of intense femtosecond pulses.

ACKNOWLEDGMENTS

This work was supported by the State Key Program for Basic Research of China under Grant No. 2012CB921500 and the National Natural Science Foundation of China (NSFC) under Grants No. 11021403, No. 10734010, No. 50771054, and No. 10804044. Partial support from NCET-08-0268 and PAPD (a project funded by the Priority Academic Program Development of Jiangsu Higher Education Institutions) is also acknowledged.

[1] V. Krylov, A. Rebane, A. G. Kalintsev, H. Schwoerer, and U. P. Wild, Opt. Lett. **20**, 198 (1995).
[2] H. Liu, J. Q. Yao, and A. Puri, Opt. Commun. **109**, 139 (1994).
[3] R. Danielius, Appl. Optics. **35**, 5336 (1996).
[4] A. Nautiyal and P. B. Bisht, Opt. Commun. **278**, 175 (2007).

[5] M. Conforti, F. Baronio, C. De Angelis, M. Marangoni, and G. Cerullo, J. Opt. Soc. Am. B **28**, 892 (2011).
[6] E. Riedle, M. Beutter, S. Lochbrunner, J. Piel, S. Schenkl, S. Sporlein, and W. Zinth, Appl. Phys. B **71**, 457 (2000).
[7] G. Cerullo, M. Nisoli, and S. De Silvestri, Appl. Phys. Lett. **71**, 3616 (1997).
[8] J. Liu, J. Zhang, and T. Kobayashi, Opt. Lett. **33**, 1494 (2008).
[9] H. P. Zeng, J. Wu, H. Xu, and K. Wu, Phys. Rev. Lett. **96**, 083902 (2006).
[10] A. Couairon and A. Mysyrowicz, Phys. Rep. **441**, 47 (2007).
[11] N. Srinivas, S. S. Harsha, and D. N. Rao, Opt. Express **13**, 3224 (2005).
[12] S. A. Ali, P. B. Bisht, A. Nautiyal, V. Shukla, K. S. Bindra, and S. M. Oak, J. Opt. Soc. Am. B **27**, 1751 (2010).
[13] S. Trillo, C. Conti, P. Di Trapani, O. Jedrkiewicz, L. Trull, G. Valiulis, and G. Bellanca, Opt. Lett. **27**, 1451 (2002).
[14] H. Zeng, J. Wu, H. Xu, K. Wu, and E. Wu, Phys. Rev. Lett. **92**, 143903 (2004).
[15] J. Bi, X. Liu, Y. H. Li, and P. X. Lu, Opt. Commun. **284**, 670 (2011).
[16] G. Wu, W. X. Li, E. Wu, and H. P. Zeng, Opt. Express **18**, 1000 (2010).
[17] C. Elliott, New J. Phys. **4**, 46 (2002).
[18] C. H. van der Wal, M. D. Eisaman, A. Andre, R. L. Walsworth, D. F. Phillips, A. S. Zibrov, and M. D. Lukin, Science **301**, 196 (2003).
[19] K. A. O'Donnell and A. B. U'Ren, Opt. Lett. **32**, 817 (2007).
[20] C. Langrock, M. Fejer, I. Hartl, and M. E. Fermann, Opt. Lett. **32**, 2478 (2007).
[21] M. Conforti, F. Baronio, and C. De Angelis, Phys. Rev. A **81**, 053841 (2010).
[22] M. Conforti, F. Baronio, and C. De Angelis, Photonics Journal, IEEE **2**, 600 (2010).
[23] R. W. Boyd, *Nonlinear Optics*, 3rd ed. (Academic Press, New York, 2003).
[24] F. Y. Sun, S. Zhang, T. L. Jia, Z. G. Wang, and Z. R. Sun, J. Opt. Soc. Am. B **26**, 549 (2009).
[25] M. Mlejnek, E. M. Wright, J. V. Moloney, and N. Bloembergen, Phys. Rev. Lett. **83**, 2934 (1999).
[26] W. H. Su, L. J. Qian, H. Luo, X. Q. Fu, H. Y. Zhu, T. Wang, K. Beckwitt, Y. F. Chen, and F. Wise, J. Opt. Soc. Am. B **23**, 51 (2006).
[27] V. Roppo, M. Centini, C. Sibilia, M. Bertolotti, D. de Ceglia, M. Scalora, N. Akozbek, M. J. Bloemer, J. W. Haus, O. G. Kosareva, and V. P. Kandidov, Phys. Rev. A **76**, 033829 (2007).
[28] M. Centini, V. Roppo, E. Fazio, F. Pettazzi, C. Sibilia, J. W. Haus, J. V. Foreman, N. Akozbek, M. J. Bloemer, and M. Scalora, Phys. Rev. Lett. **101**, 113905 (2008).
[29] E. Fazio, F. Pettazzi, M. Centini, M. Chauvet, A. Belardini, M. Alonzo, C. Sibilia, M. Bertolotti, and M. Scalora, Opt. Express **17**, 3141 (2009).
[30] E. T. J. Nibbering, P. F. Curley, G. Grillon, B. S. Prade, M. A. Franco, F. Salin, and A. Mysyrowicz, Opt. Lett. **21**, 62 (1996).
[31] E. Yablonovitch, Phys. Rev. Lett. **32**, 1101 (1974).
[32] E. Yablonovitch, Phys. Rev. A **10**, 1888 (1974).
[33] J. Liu, H. Schroeder, S. Chin, R. Li, and Z. Xu, Opt. Express **13**, 10248 (2005).
[34] A. Brodeur and S. L. Chin, Phys. Rev. Lett. **80**, 4406 (1998).
[35] G. G. Luther, A. C. Newell, J. V. Moloney, and E. M. Wright, Opt. Lett. **19**, 789 (1994).
[36] M. Kolesik, E. M. Wright, and J. V. Moloney, Phys. Rev. Lett. **92**, 253901 (2004).
[37] H. DiLorenzo Pires, F. M. G. J. Coppens, and M. P. van Exter, Phys. Rev. A **83**, 033837 (2011).
[38] P. S. K. Lee, M. P. van Exter, and J. P. Woerdman, Phys. Rev. A **72**, 033803 (2005).
[39] R. M. Rassoul, A. Ivanov, E. Freysz, A. Ducasse, and F. Hache, Opt. Lett. **22**, 268 (1997).
[40] M. Goul'kov, S. Odoulov, I. Naumova, F. Agullo-Lopez, G. Calvo, E. Podivilov, B. Sturman, and V. Pruneri, Phys. Rev. Lett. **86**, 4021 (2001).
[41] M. Goulkov, O. Shinkarenko, L. Ivleva, P. Lykov, T. Granzow, T. Woike, M. Imlau, and M. Wohlecke, Phys. Rev. Lett. **91**, 243903 (2003).
[42] H. Tan, G. P. Banfi, and A. Tomaselli, Appl. Phys. Lett. **63**, 2472 (1993).
[43] S. X. Dou, D. Josse, and J. Zyss, J. Opt. Soc. Am. B **8**, 1732 (1991).
[44] S. L. Chin, A. Brodeur, S. Petit, O. G. Kosareva, and V. P. Kandidov, J. Nonlinear. Opt. Phys. **8**, 121 (1999).